physica status solidi

pss

www.pss-journals.com

reprint

WILEY-VCH

Phys. Status Solidi A, 1–6 (2011) / **DOI** 10.1002/pssa.201127403

physica status solidi a
www.pss-a.com
applications and materials science

Ferromagnetism in rare earth doped cerium oxide bulk samples

M. Chandra Dimri*[,1], H. Khanduri[1,2], H. Kooskora[1], J. Subbi[1], I. Heinmaa[1], A. Mere[2], J. Krustok[2], and R. Stern[1]

[1] National Institute of Chemical Physics and Biophysics, Tallinn 12618, Estonia
[2] Tallinn University of Technology, Tallinn 19086, Estonia

Received 11 July 2011, revised 28 October 2011, accepted 3 November 2011
Published online 24 November 2011

Keywords ferro- and paramagnetism, rare-earth doped ceria, spintronics, susceptibility

* Corresponding author: e-mail mukeshdimri@yahoo.com, Phone: +3726398370, Fax: +3726703662

Magnetic properties of rare earth (RE) doped ceria (RE = Nd, Sm, Gd, Tb, Er and Dy) samples have been investigated and reported in this paper. Room temperature ferromagnetism (FM) was observed in calcined powders as well as in sintered samples of Nd and Sm doped CeO_2, whereas other RE dopants (Gd, Tb, Er and Dy) in CeO_2 exhibit paramagnetic behaviour. The origin of magnetism in these samples can be related to oxygen vacancies and formation of fluorite crystal structure. Though the magnetization was found to be lower as compared to transition metal (TM) doped ceria, the segregation of metallic and secondary phases can be avoided in RE doped CeO_2. CeO_2 doped with Sm ions in different concentration (1, 5 and 15%) were also studied to see the dopant effects on magnetic properties. The origin of magnetism in these samples may be related to the oxygen vacancies created due to RE dopants, which was confirmed from the peak around 555 cm^{-1} in Raman spectra.

1 Introduction Dilute magnetic semiconductors (DMS) have drawn considerable attention due to their projected applications in spintronic devices [1, 2]. Transition metal (TM) doping has been proposed to introduce magnetic functionality in conventional semiconductors and metal oxides. A great deal of investigations have been carried out on semiconductors or insulators doped with TMs, and ferromagnetism (FM) with high Curie temperature (T_c) was obtained in some doped oxides such as ZnO, TiO_2, SnO_2, ZrO_2, HfO_2 and CeO_2 [3–8]. The real origin of magnetism is still doubtful in most of these studies. In some cases, it was demonstrated that the FM is due to segregation of metallic clusters, while in some systems it is because of different valance state of TM. CeO_2 is paramagnetic at ambient temperature and used as a key material in high K capacitors and as buffer layer in silicon on insulator devices [9–12]. Since CeO_2 is a face-centred cubic system possessing a fluorite crystal structure with closely matched lattice parameters to silicon, it has potential to facilitate the integration of next generation spintronic devices with current silicon based microelectronic devices. So existence of magnetism in this material would create a new direction for potential spintronic devices. However, there are some reports on magnetic properties of CeO_2 in nano form [13, 14], and doped with non-magnetic ions, such as calcium [15] as well as doped with TMs [13, 16–19]. But there are always problems of reproducibility or precipitation of secondary metallic phase in TM doped oxides. The problems related to phase segregation could be overcome in case of rare earth (RE) doped ceria, those are well-studied material for other technological applications such as fuel cells, oxygen sensors, catalysis *etc*. [16, 20–23]. The addition of RE ions to CeO_2 results in solid solutions of the form $Ce_{1-x}RE_xO_{2-\delta}$ that have the same fluorite structure as does CeO_2 upto a large atomic fraction of RE metals [24, 25]. To the best of our knowledge there are no reports on magnetic behaviour of RE doped CeO_2 powders and bulk samples.

Our objectives were to synthesize various RE (Nd, Sm, Gd, Tb, Dy and Er) doped CeO_2 samples and investigate their magnetic properties. It is interesting to note that Nd and Sm doped CeO_2 powders as well as sintered samples show magnetic hysteresis at room temperature, whereas other dopants (Gd, Tb, Er and Dy) in CeO_2 exhibit paramagnetic behaviour. This abnormal behaviour has been related to the change in crystal structure and oxygen vacancies created on RE doping in ceria.

2 Experimental Polycrystalline samples of 20 at.% RE (Nd, Sm, Tb, Dy and Er) doped CeO_2 powders ($Ce_{0.8}RE_{0.2}O_{2-\delta}$) were prepared by chemical solution

method. Metal nitrates and oxides were used as starting material to prepare the 0.5 M solution in deionized (DI) water. The purity of RE oxides (Sm_2O_3 and Nd_2O_3 *etc.*) obtained from Fluka chemicals, were 99.9%, and remaining 0.1% were also RE oxide impurities. So there is not any possibility of insertion of magnetic ion impurity (such as Fe, Co *etc.*) from the starting materials. Citric acid was used as combustion agent and 0.5 M solution in DI water was added in 3:2 for every cation. After mixing the solutions, resulting solution was dried at 80 °C and later calcined at 800 °C for 5 h in air. These powders were pressed in disc shape pellets and sintered at different temperatures (1350–1500 °C) for 3 h in air to form the compact fluorite structured ceria. Commercial nanopowders (average particle sizes in range 5–10 nm) of 10% gadolinium doped ceria (GDC10) from Praxair speciality ceramics (purity 99.9%) were also sintered at 1500 °C/3 h. Lower percentages (1, 5 and 15 at.%) of samarium doped CeO_2 samples were also prepared using the same method described above, to compare the dopant effects on magnetic properties. RIGAKU Ultima IV X-ray diffractometer was used for structural characterization, whereas Raman spectra at room temperature were recorded by Horiba Jobin Yvon LabRAM HR 800 spectrometer. A commercial vibrating sample magnetometer option in 14T-PPMS (Quantum Design) was used for the measurements of temperature and field dependence of magnetic susceptibility.

3 Results and discussions Figure 1 shows the X-ray diffractograms for different RE doped ceria samples. All of the powders show characteristic diffraction peaks corresponding to fluorite structure of CeO_2 [26], without extra segregated metal ion peaks. There are minor shifts in the peak position due to different ionic radii of RE dopants, and the peaks are broader for the powders heated at 800 °C, which may be due to smaller particles at this temperature.

Raman spectra measured at room temperature for different $Ce_{1-x}RE_xO_2$ bulk samples are shown in Fig. 2(a). All spectra except Er doped CeO_2 show F_{2g} Raman peak around 465 cm^{-1}, which is the characteristic peak for fluorite structured cerium oxide [27, 28]. Sm and Nd doped ceria samples show other broad peak around 555 cm^{-1}, which has been assigned to the oxygen vacancies originating from the

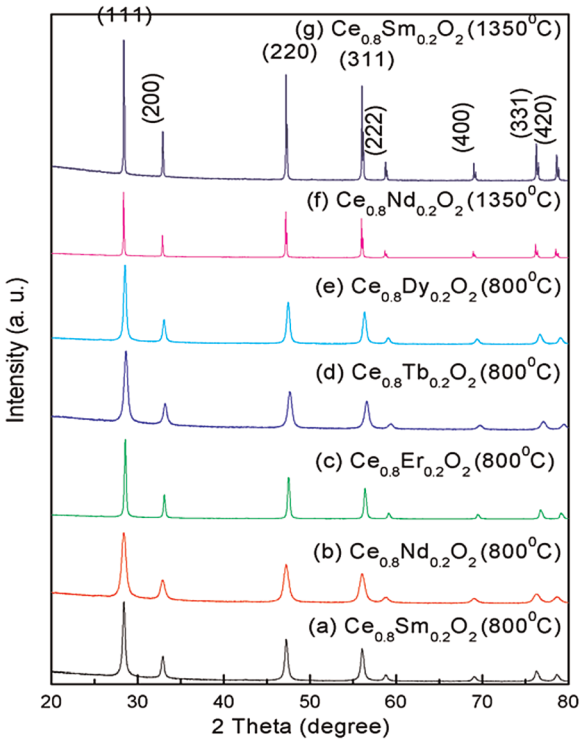

Figure 1 (online colour at: www.pss-a.com) XRD patterns of $Ce_{0.8}RE_{0.2}O_{2-\delta}$ powder and sintered samples.

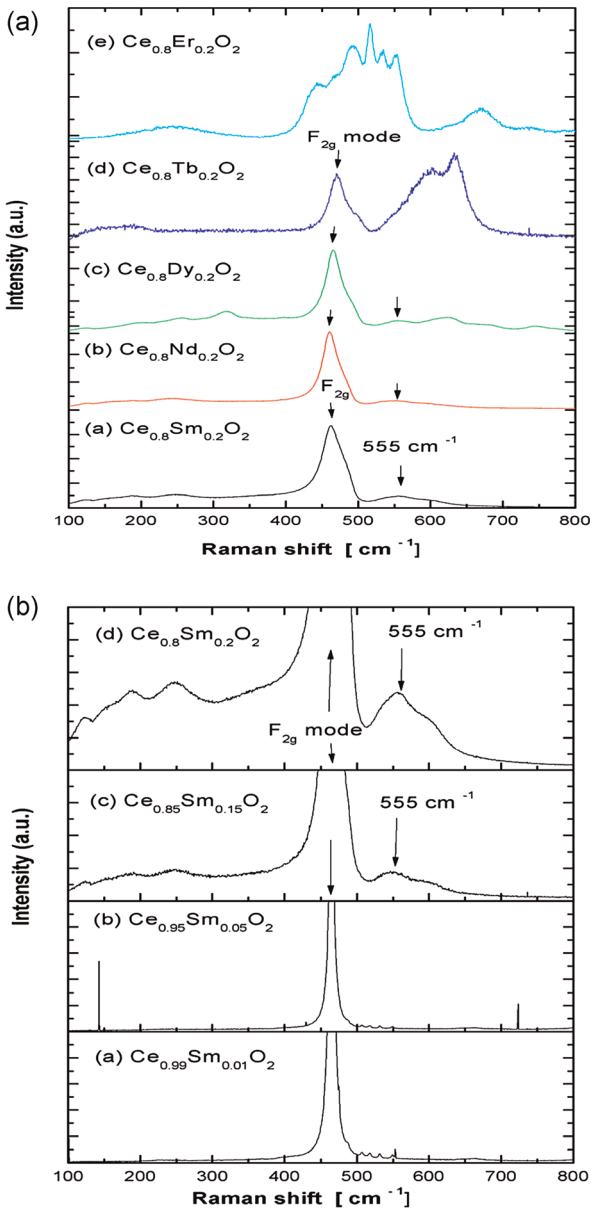

Figure 2 (online colour at: www.pss-a.com) Raman spectra of (a) 20 at.% RE (RE = Sm, Dy, Tb, Nd, Er) doped ceria and (b) 1, 5, 15 and 20 at.% Sm doped CeO_2 sintered samples.

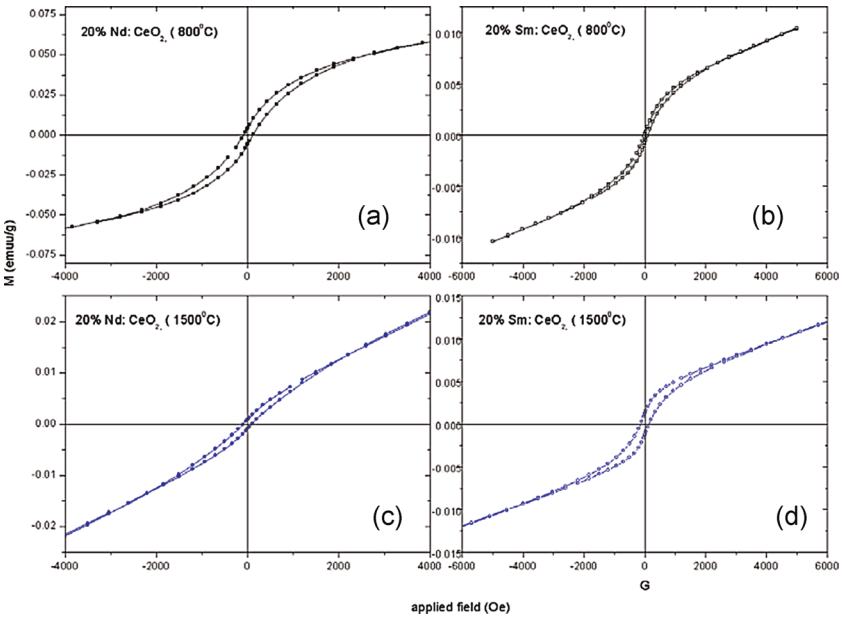

Figure 3 (online colour at: www.pss-a.com) Hysteresis loops measured at 300 K; (a) 20% Nd doped CeO_2 powders heated at 800 °C, (b) 20% Sm doped CeO_2 powders heated at 800 °C, (c) 20% Nd doped CeO_2 powders heated at 1500 °C, (d) 20% Sm doped CeO_2 powders heated at 1500 °C.

RE substitution in ceria [24, 29]. Tb and Er doped samples have additional Raman modes as compared to Nd, Dy and Sm doped ceria samples. The difference in Raman spectra was also exhibited in different magnetic properties, which will be discussed in magnetic section of this paper. Figure 2(b) shows the Raman spectra for different at.% of Sm doped ceria with two distinct peaks around 465 and 555 cm^{-1}. The intensity of the peak arising due to oxygen vacancies (~555 cm^{-1}) starts growing on increasing the Sm concentration in ceria, suggesting higher oxygen vacancies on substitution with Sm ions.

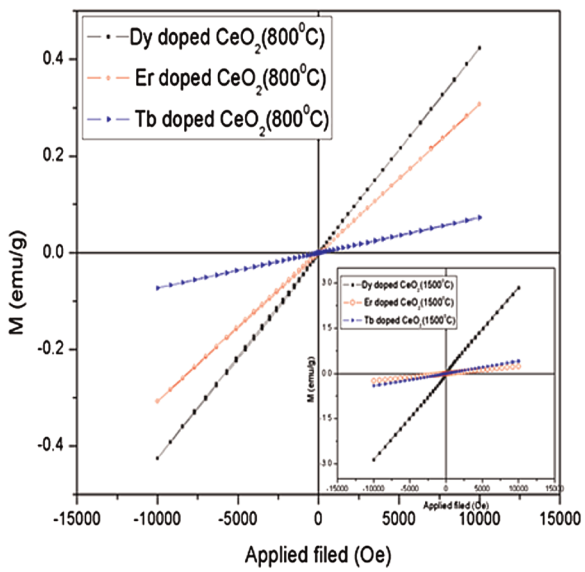

Figure 4 (online colour at: www.pss-a.com) Hysteresis loops measured at 300 K for Dy, Er and Tb doped CeO_2 powders heated at 800 °C (inset picture shows loops for sintered samples at 1500 °C).

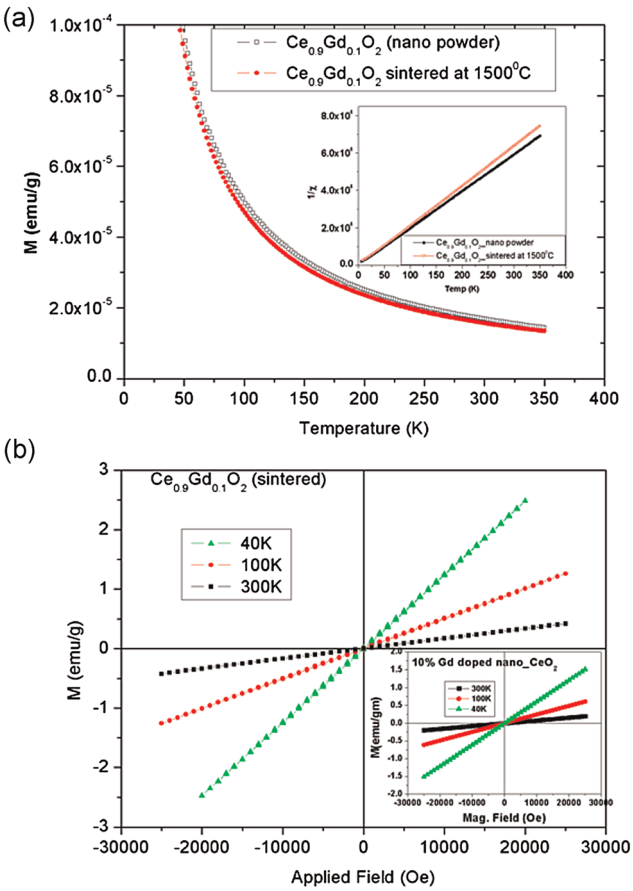

Figure 5 (online colour at: www.pss-a.com) (a) Susceptibility and inverse susceptibility (inset) curves for nanopowders and sintered samples of $Ce_{0.9}Gd_{0.1}O_2$; (b) *M–H* curves for sintered sample of $Ce_{0.9}Gd_{0.1}O_2$ (nanopowders in inset).

Figure 3(a) and (b) show hysteresis loops measured at 300 K for 20% Nd and Sm doped CeO_2 powders (calcined at 800 °C/5 h), whereas Fig. 3(c) and (d) show those for the corresponding sintered samples (1500 °C/3 h). *M–H* curves for 20% Dy, Er and Tb doped CeO_2 powder samples (heated at 800 °C/5 h) are shown in Fig. 4, and the inset picture shows those for corresponding sintered samples (1500 °C/3 h). From these figures it can be seen that Nd and Sm doped samples exhibit hysteresis at room temperature as compared to other samples, which show paramagnetic behaviour. It is clear from these hysteresis curves that Nd and Sm doped CeO_2 sintered samples have ferromagnetic behaviour in addition to some linear paramagnetic signal. This behaviour may be related to the phase purity, which can be seen in extra peaks of Raman spectra shown in Fig. 2(a). The Raman spectra for the Nd and Sm doped ceria show peaks for fluorite structure and oxygen vacancies, whereas other samples have extra peaks of cubic ceria (not detected in XRD pattern) and RE oxides. No saturation was observed in measured *M–H* curves due to the paramagnetic contributions. Usually the FM have been observed in CeO_2 samples due to surface defects in nanoparticles [13, 14], but in our samples it was found in bulk-sintered samples as well.

Figure 5(a) shows the variation of magnetic susceptibility with temperature for commercial $Ce_{0.9}Gd_{0.1}O_2$ nanopowders and its sintered samples. Temperature dependence of susceptibility exhibits the Curie type paramagnetic behaviour in these samples. *M–H* loops measured at different temperatures with a maximum field of 2.5 kOe are shown in Fig. 5(b), which also confirms the paramagnetic behaviour in nano as well as sintered $Ce_{0.9}Gd_{0.1}O_2$ samples. Bulk Gd is ferromagnetic with a Curie temperature ~300 K, but it could not help in getting FM in 10 at.% Gd doped CeO_2 samples.

Figure 6(a) show hysteresis loops measured at 300 K for 20 at.% Sm doped CeO_2 sintered samples (1350 and 1500 °C/3 h). From the as measured curves, we can see that there is linear paramagnetic contribution in addition to ferromagnetic signal, and no saturation of magnetization obtained upto an applied magnetic field of 25 kOe. The magnetization is lower in sample sintered at 1350 °C, as compared to that sintered at 1500 °C, which can be seen from the paramagnetic subtracted curves (inset picture). The corecivities estimated from the hysteresis curves were 75 and 30 Oe for the $Ce_{0.8}Sm_{0.2}O_2$ powders sintered at 1350 and 1500 °C, respectively. The hysteresis loops (after subtracting paramagnetic straight line) measured at 300 K, are shown in Fig. 6(b) for different at.% of Sm doped CeO_2 sintered samples. Saturation magnetization increases with the increase in Sm concentration in these samples, which may be related to more oxygen vacancies created due to RE doping, confirmed from the Raman spectra shown in Fig. 2(b).

Temperature dependence of susceptibility for the calcined powders (800 °C) and sintered bulk samples of $Ce_{0.8}Sm_{0.2}O_2$ are shown in Fig. 7. The magnetization signal was found to be noisy (weak) for the powders at high temperatures. The inset picture in Fig. 7 shows the temperature dependence of susceptibilities of sintered

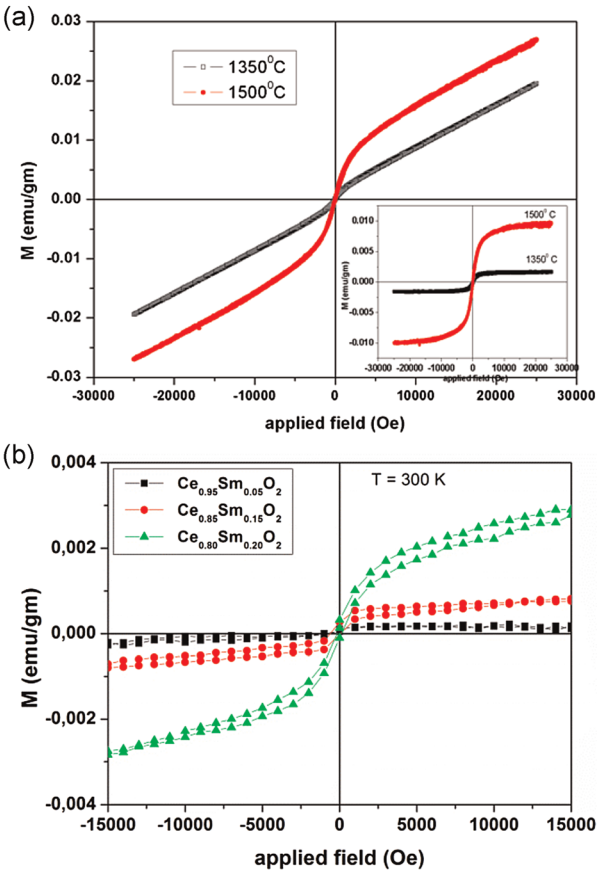

Figure 6 (online colour at: www.pss-a.com) (a) Magnetization (*M*) *versus* magnetic field (*H*) as measured at 300 K, for $Ce_{0.8}Sm_{0.2}O_2$ sintered samples, inset picture shows the paramagnetic subtracted curves. (b) Subtracted *M–H* curves for $Ce_{1-x}Sm_xO_2$ ($x = 0.05$, 0.15 and 0.20) samples sintered at 1500 °C/3 h.

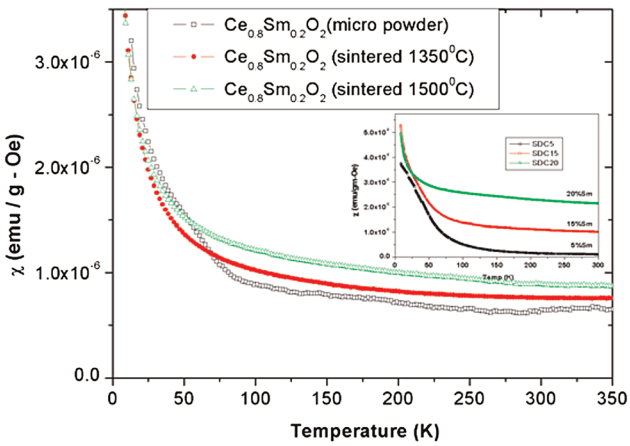

Figure 7 (online colour at: www.pss-a.com) Temperature dependence of susceptibility for the micro sized powders and sintered samples of $Ce_{0.8}Sm_{0.2}O_2$ (inset picture shows susceptibilities of sintered CeO_2 samples doped with different samarium concentration).

CeO_2 samples doped with different samarium concentration (5, 15 and 20 at.%). The magnetic moment for 1 at.% Sm doped ceria sample was very weak (not included in the figures). There is increase in magnetization (susceptibilities) because of higher oxygen vacancies with the increase in Sm concentration from 5 to 20 at.%. The temperature dependence is like Curie–Weiss type, with no magnetic transitions in the measured temperature range.

Usually the magnetic ordering in insulating materials is caused by superexchange coupling, but the coupling results in antiferromagnetic ordering [16, 30]. It is well known that cerium in CeO_2, can be in Ce^{+3} or Ce^{+4} valance states, whereas RE ions are generally found in RE^{+3} valance state [31]. So substitution with RE ions should create more oxygen vacancies [24], and finally to enhance the FM. There are few studies on FM in RE doped ZnO caused by s–f coupling [32, 33]. But there is absence of FM at room temperature in most of our RE doped ceria samples (except Nd and Sm doped), as can be seen from the magnetic hysteresis loops (Figs. 3 and 4). The RE metals Nd and Sm have 3 and 5 unpaired electrons in their 4f shell, whereas Gd has 7 unpaired electrons in 4f shell. It is surprising to note that Gd is well ferromagnetic at room temperature and has half filled 4f shell (7 unpaired electrons), even it could not produce ferromagnetic ordering either via s–f coupling or F-centre mediated exchange mechanism, however, it enhanced the magnetic moment per Gd atom. La doped CeO_2 show very weak magnetic signal (not included in this paper), and there was no sign of FM in the sintered powders of the samples of different percentage of lanthanum in CeO_2. The weak magnetic behaviour in La doped samples can be understood because of vacant f orbital, but we do not understand the magnetic behaviour in other doped samples on basis of unpaired electron in 4f shell. One reason may be due to orbital moment quenching of RE ions in these oxides. Orbital quenching of TM ions due to crystal field splitting is a well-known phenomenon in TM oxides, but in this case orbital quenching occurs in RE ions. Though the origin of magnetism is still debatable in these oxides, but in our samples the origin of magnetism seems to be due to oxygen vacancies created by RE dopants, and not because of metal ions segregation.

4 Conclusions Magnetic studies on powder and sintered samples of RE doped CeO_2 show that Nd and Sm doped CeO_2 samples exhibit FM at room temperature, whereas other dopants (La, Gd, Er, Tb and Dy) could not produce the long-range FM in CeO_2 samples. The FM observed in these doped CeO_2 samples cannot be related to surface defects observed in nanoparticles, but it is found in bulk-sintered samples as well. The cause of magnetism may be due to oxygen vacancies created by RE dopants in ceria, which was confirmed from the Raman spectra. Also the problem of metallic phase segregation in these RE doped ceria can be avoided, which is generally observed in TM doped oxides. The observation of FM in RE doped high K dielectric ceramic material may have potential application in field of spintronics.

Acknowledgements This work was financially supported by Estonian Science Foundation (grant numbers: MJD 65 and ETF 8440), and Estonian targeted financial grants SF0690029s09 and SF0690034s09.

References

[1] H. Ohno, Science **281**, 951 (1998).
[2] T. Dietl, H. Ohno, F. Matsukura, J. Cibert, and D. Ferrand, Science **287**, 1019 (2000).
[3] M. Venkatesam, C. B. Fitzgerald, J. G. Lunney, and J. M. D. Coey, Phys. Rev. Lett. **93**, 177206 (2004).
[4] Z. L. Lu, W. Miao, W. Q. Zou, M. X. Xu, and F. M. Zhang, J. Alloys Compd. **494**, 392 (2010).
[5] N. H. Hong, J. Sakai, W. Prellier, A. Hassini, A. Ruyter, and F. Gervais, Phys. Rev. B **70**, 195204 (2004).
Z. M. Tian, S. L. Yuan, J. H. He, P. Li, S. Q. Zhang, C. H. Wang, Y. Q. Wang, S. Y. Yin, and L. Liu, J. Alloys Compd. **466**, 26 (2008).
[6] J. M. D. Coey, A. P. Douvalis, C. B. Fitzgerald, and M. Venkatesan, Appl. Phys. Lett. **84**, 1332 (2004).
[7] M. C. Dimri, H. Kooskora, J. Pahapill, E. Joon, I. Heinmaa, J. Subbi, and R. Stern, Phys. Status Solidi A **208**(1), 172 (2011).
[8] N. H. Hong, J. Sakai, W. Prellier, and A. Hassini, J. Phys.: Condens. Matter **17**, 1697 (2005).
[9] A. Thurber, K. M. Reddy, V. Shutthanandan, M. H. Engelhard, C. Wang, J. Hays, and A. Punnoose, Phys. Rev. B **76**, 165206 (2007).
[10] T. Inoue, T. Ohsuna, L. Luo, X. D. Wu, C. J. Maggiore, Y. Yamamoto, Y. Sakurai, and J. H. Chang, Appl. Phys. Lett. **59**, 3604 (1991).
[11] Y. Nishikawa, T. Yamaguchi, M. Yoshiki, H. Satake, and N. Fukushima, Appl. Phys. Lett. **81**, 4386 (2002).
[12] J. Kang, X. Liu, G. Lian, Z. Zhang, G. Xiong, X. Guan, R. Han, and Y. Wang, Microelectron. Eng. **56**, 191 (2001).
[13] Q. Y. Wen, H. W. Zhang, Y. Q. Song, Q. H. Yang, H. Zhu, and J. Q. Xiao, J. Phys.: Condens. Matter **19**, 246205 (2007).
[14] M. Y. Ge, H. Wang, E. J. Liu, J. F. Liu, J. Z. Jiang, Y. K. Li, A. Z. Xu, and H. Y. Li, Appl. Phys. Lett. **93**, 062505 (2008).
[15] X. Chen, G. Li, Y. Su, X. Qiu, L. Li, and Z. Zou, Nanotechnology **20**, 115606 (2009).
[16] A. Tiwari, V. M. Bhosle, S. Ramachandran, N. Sudhakar, J. Narayan, S. Budak, and A. Gupta, Appl. Phys. Lett. **88**, 142511 (2006).
[17] M. Santi, P. Sumalin, L. Paveena, and S. Supapan, J. Nanosci. Nanotechnol. **9**(11), 6415 (2009).
[18] L. R. Shah, B. Ali, H. Zhu, W. G. Wang, Y. Q. Song, H. W. Zhang, S. I. Shah, and J. Q. Xiao, J. Phys.: Condens. Matter **21**, 486004 (2009).
[19] C. Xia, C. Hu, P. Chen, B. Wan, X. He, and Y. Tian, Mater. Res. Bull. **45**, 794 (2010).
[20] T. S. Stefanic and H. L. Tuller, J. Eur. Ceram. Soc. **21**, 1967 (2001).
[21] S. Park, J. M. Vohs, and R. J. Gorte, Nature **404**, 265 (2000).
[22] G. A. Delug, J. R. Salge, L. D. Schmidt, and X. E. Verykios, Science **303**, 933 (2004).
[23] K. Otsuka, T. Ushiyama, and I. Yamanaka, Chem. Lett. **22**, 1517 (1993).

[24] J. R. McBride, K. C. Hass, B. D. Poindexter, and W. H. Weber, J. Appl. Phys. **76**, 2435 (1994).
[25] J.-G. Li, Y. Wang, T. Ikegami, T. Mori, and T. Ishigaki, Mater. Sci. Eng. B **121**, 54 (2005).
[26] H. Nitani, T. Nakagawa, M. Yamanouchi, T. Osuki, M. Yuya, and T. A. Yamamoto, Mater. Lett. **58**, 2076 (2004).
[27] W. H. Weber, K. C. Hass, and J. R. McBride, Phys. Rev. B **48**, 178 (1993).
[28] Z. D. Dohčević-Mitrović, M. J. Šćepanović, M. U. Grujić-Brojčin, Z. V. Popović, S. B. Bošković, B. M. Matović, M. V. Zinkevich, and F. Aldinger, Solid State Commun. **137**, 387 (2006).
[29] M. D. Hernandez-Alonso, A. B. Hugria, A. Martinez-Arias, J. M. Coronado, J. C. Conesa, J. Soria, and M. Fernandez-Garcia, Phys. Chem. Chem. Phys. **6**, 3524 (2004).
[30] J. M. D. Coey, M. Venkatesan, and C. B. Fitzgerald, Nature Mater. **4**, 173 (2005).
[31] F. Ye, T. Mori, D. R. Ou, G. Auchterlonie, J. Zou, and J. Drennan, J. Appl. Phys. **101**, 113528 (2007).
[32] H. Shi, P. Zhang, S. S. Li, and J. B. Xia, J. Appl. Phys. **106**, 023910 (2009).
[33] K. Potger, S. Zhou, F. Eichhorm, M. Helm, W. Skorupa, A. Mcklich, J. Fassbender, T. Hermannsdorfer, and A. Bianchi, J. Appl. Phys. **99**, 063906 (2006).

